PHYSICAL REVIEW D **91,** 035010 (2015)

# One-loop SQCD corrections to the decay of top squarks to charm and neutralino in the generic MSSM

Jason Aebischer,[1,*] Andreas Crivellin,[2,†] and Christoph Greub[1,‡]

[1]*Albert Einstein Center for Fundamental Physics, Institute for Theoretical Physics, University of Bern, CH-3012 Bern, Switzerland*

[2]*CERN Theory Division, CH-1211 Geneva 23, Switzerland*

(Received 4 November 2014; published 11 February 2015)

In this article we calculate the one-loop supersymmetric QCD (SQCD) corrections to the decay $\tilde{u}_1 \to c\tilde{\chi}_1^0$ in the minimal supersymmetric standard model with generic flavor structure. This decay mode is phenomenologically important if the mass difference between the lightest squark $\tilde{u}_1$ (which is assumed to be mainly stoplike) and the neutralino lightest supersymmetric particle $\tilde{\chi}_1^0$ is smaller than the top mass. In such a scenario $\tilde{u}_1 \to t\tilde{\chi}_1^0$ is kinematically not allowed and searches for $\tilde{u}_1 \to Wb\tilde{\chi}_1^0$ and $\tilde{u}_1 \to c\tilde{\chi}_1^0$ are performed. A large decay rate for $\tilde{u}_1 \to c\tilde{\chi}_1^0$ can weaken the LHC bounds from $\tilde{u}_1 \to Wb\chi_1^0$ which are usually obtained under the assumption $\mathrm{Br}[\tilde{u}_1 \to Wb\chi_1^0] = 100\%$. We find the SQCD corrections enhance $\Gamma[\tilde{u}_1 \to c\tilde{\chi}_1^0]$ by approximately 10% if the flavor violation originates from bilinear terms. If flavor violation originates from trilinear terms, the effect can be $\pm 50\%$ or more, depending on the sign of $A^t$. We note that connecting a theory of supersymmetry breaking to LHC observables, the shift from the $\overline{\mathrm{DR}}$ to the on-shell mass is numerically very important for light stop decays.

DOI: 10.1103/PhysRevD.91.035010 PACS numbers: 12.60.Jv



## I. INTRODUCTION

Natural supersymmetry requires light stops in order to cancel the quadratic divergences of the Higgs self-energies involving a top quark while the other supersymmetric partner can be much heavier [1,2]. Theoretical motivation for light stops also comes from the fact that when starting at a high scale with universal squark masses, the renormalization group evolution (RGE) (known at the two-loop level [3–5]) generically drives the masses of the third generation squarks to lower values as for example in gravity mediated supersymmetry (SUSY)-breaking scenarios (see for example [6]). In addition, light stops are also welcome in order to accommodate for the observed relic density within the minimal supersymmetric standard model (MSSM) [7–12] and to realize baryogenesis [13–21].

On the experimental side, the bounds on the stop mass are much weaker than the ones on the other strongly interacting SUSY particles, i.e. squarks of the first two generations [22,23] and the gluino (see for example [24] for a recent overview of ATLAS and CMS results). Light stops might even be welcome in the light of recent LHC data for $W$-pair production where the observed cross section [25,26] is slightly above the standard model (SM) predictions [27]. This can be interpreted as a hint for light sleptons, light charginos and/or light stops [28,29]. However, in order to accommodate the measured Higgs mass of around 125 GeV [30,31] rather heavy stops are required. This tension can be solved if the stop-mixing angle is large (or even maximal [32]), by promoting the MSSM to the next-to-minimal supersymmetric standard model (NMSSM) or $\lambda$SUSY [33,34] or by adding D-term contributions [35].

Concerning the exclusion limits on stop masses from the LHC, there are still regions in parameter space in which light stops are allowed. If the mass splitting between the stop and the neutralino is bigger than the top mass, the main search channel is $\tilde{u}_1 \to t\tilde{\chi}_1^0$ and the constraints are stringent [36,37]. However, if the mass difference is smaller than $m_t$ the limits on the stop mass come from searches for $\tilde{u}_1 \to Wb\tilde{\chi}_1^0$ and the limits are much weaker [38–41]. If the mass difference between the stop and the neutralino is even smaller than $m_W + m_b$ the limits are obtained from searches for the flavor-changing decay $\tilde{u}_1 \to c\tilde{\chi}_1^0$ [42,43].

The decay $\tilde{u}_1 \to c\tilde{\chi}_1^0$ has important experimental implications, both for scenarios with minimal and nonminimal flavor violation.

In the case of minimal flavor violation [44–48] the decay rate is suppressed leading to a sizable stop decay length, which can be used to determine the flavor structure [49,50] and is in principle measurable at the LHC [51–54].[1] The most plausible scenario with a suppressed stop decay rate $\tilde{u}_1 \to c\tilde{\chi}_1^0$ is to assume a flavor-blind SUSY-breaking

*aebischer@itp.unibe.ch
†andreas.crivellin@cern.ch
‡greub@itp.unibe.ch



[1]If the decay rate for $\tilde{u}_1 \to c\tilde{\chi}_1^0$ is small, the four-body decay $\tilde{u}_1 \to b\tilde{\chi}_1^0 f f'$ [55] (also searched for at the LHC [40]) can have a significant impact on the branching ratio for $\tilde{u}_1 \to c\tilde{\chi}_1^0$ [56].

mechanism at some high scale $\Lambda$, for example the grand unified theory (GUT) scale. In this case, flavor off-diagonal elements in the squark mass matrices are induced by the renormalization group for which the decay width has been calculated in Ref. [57] and the finite part of the one-loop electroweak corrections has been computed in Ref. [56].[2]

In the case of nonminimal flavor violation the decay width for $\tilde{u}_1 \to c\tilde{\chi}_1^0$ can be significantly enhanced since the flavor-changing elements in the up sector are rather poorly constrained from flavor changing neutral current processes. It has been noticed in Ref. [62] (see also [63,64] for later analysis) that an enhanced branching ratio for $\tilde{u}_1 \to c\tilde{\chi}_1^0$ can weaken the bounds from $\tilde{u}_1 \to t\tilde{\chi}_1^0$, for which a branching ratio of 100% is commonly assumed in the experimental analysis, allowing for lighter stop masses. We point out that a similar effect occurs concerning the limits extracted from $\tilde{u}_1 \to Wb\chi_1^0$ searches. Since $\tilde{u}_1 \to Wb\chi_1^0$ is a three-body decay, it is kinematically suppressed compared to the two-body decay $\tilde{u}_1 \to t\tilde{\chi}_1^0$. Therefore, already a much smaller amount of flavor violation, as the one necessary to affect the limits from $\tilde{u}_1 \to t\tilde{\chi}_1^0$, would be sufficient to significantly weaken the limits extracted from $\tilde{u}_1 \to Wb\chi_1^0$. This observation is especially interesting taking into account that the bounds on the stop mass from $\tilde{u}_1 \to Wb\chi_1^0$ are currently anyway the weakest ones. Therefore, very light stop masses for $m_W < m_{\tilde{u}_1} - m_{\tilde{\chi}^0} < m_t$ are allowed, especially in the case of nonminimal flavor violation.

In this article we investigate the one-loop supersymmetric QCD (SQCD) corrections to $\tilde{u}_1 \to c\tilde{\chi}_1^0$ in the MSSM[3] with generic flavor structure. These $\alpha_s$ corrections are the leading ones in the case of nonminimal flavor violation. Furthermore, assuming a flavor-blind SUSY-breaking mechanism at a high scale $\Lambda$ the counting of the loop effects is as follows: The leading order effect is the one-loop electroweak running from $\Lambda$ to $m_{\mathrm{SUSY}}$. To this leading effect the next-to-leading order (NLO) corrections are the two-loop RGE effects [3–5] originating from $\alpha_s$ and the one-loop QCD corrections to the decay width at the SUSY scale which we calculate here.[4]

The article is structured as follows: In the next section we establish our conventions and recall the tree-level expression for the decay rate for $\tilde{u}_1 \to c\tilde{\chi}_1^0$. Section III describes the calculation as well as the renormalization followed by a numerical analysis in Sec. IV. Finally we conclude in Sec. V.

[2]The corresponding corrections for the flavor conserving case were calculated in Refs. [58–61].

[3]Even though we refer to the MSSM here, our analysis does not depend on the Higgs sector of the MSSM and thus also applies to nonminimal extensions like the NMSSM and $\lambda$SUSY [33,34].

[4]This work was presented at the SUSY conference [65]. During completion of our work the SUSY-QCD corrections to the decay $\tilde{t} \to c\tilde{\chi}_1^0$ have been presented for the first time [66]. In that paper furthermore a phenomenological analysis including the flavor-changing two-body decay of the lightest stop into a charm quark and the lightest neutralino and its four-body decay into the lightest neutralino, a down-type quark and a fermion pair, has been performed. However, Ref. [66] uses a different renormalization scheme than we do.

## II. CONVENTIONS AND TREE-LEVEL DECAY

In this section we define our conventions and discuss the tree-level decay width. First, we denote the term in the Lagrangian for the coupling of an up quark $u_i$ to an up squark $\tilde{u}_s$ and a neutralino $\tilde{\chi}_p^0$ as

$$\tilde{u}_s^* \bar{\tilde{\chi}}_p^0 \left[ \Gamma_{\tilde{u}_s u_i}^{\tilde{\chi}_p^0 L} P_L + \Gamma_{\tilde{u}_s u_i}^{\tilde{\chi}_p^0 R} P_R \right] u_i + \text{H.c.}, \tag{1}$$

where $P_L$ and $P_R$ are chiral projectors. For the coupling of quarks to squarks and gluinos we introduce a similar notation:

$$\tilde{u}_s^* \bar{\tilde{g}} \left[ \Gamma_{\tilde{u}_s u_i}^{\tilde{g} L} P_L + \Gamma_{\tilde{u}_s u_i}^{\tilde{g} R} P_R \right] u_i + \text{H.c.} \tag{2}$$

In the following, we will order the mass eigenstates for the neutralino $p = 1$–$4$ and of the up squarks $s = 1$–$6$ in increasing order and $u_3$, $u_2$ and $u_1$ correspond to the $t$, $c$ and $u$ quark, respectively. For the neutralino mass matrix we use the convention

$$\mathcal{M}_{\tilde{\chi}^0} = \begin{pmatrix} M_1 & 0 & \frac{-v_d g_1}{\sqrt{2}} & \frac{v_u g_1}{\sqrt{2}} \\ 0 & M_2 & \frac{v_d g_2}{\sqrt{2}} & \frac{-v_u g_2}{\sqrt{2}} \\ \frac{-v_d g_1}{\sqrt{2}} & \frac{v_d g_2}{\sqrt{2}} & 0 & -\mu \\ \frac{v_u g_1}{\sqrt{2}} & \frac{-v_u g_2}{\sqrt{2}} & -\mu & 0 \end{pmatrix}, \tag{3}$$

with $v = \sqrt{2} m_W / g_2 \approx 174$ GeV and $v_u / v_d = \tan\beta$. $M_1$ and $M_2$ denote the gaugino masses and $\mu$ is the higgsino mass. The up-squark mass term in the Lagrangian is given by

$$-( \tilde{u}_L^* \quad \tilde{u}_R^* ) \mathcal{M}_u^2 \begin{pmatrix} \tilde{u}_L \\ \tilde{u}_R \end{pmatrix}, \tag{4}$$

where both $\tilde{u}_L$ and $\tilde{u}_R$ are three-vectors in flavor space. The squark mass(-squared) matrix is given by

$$\mathcal{M}_{\tilde{u}}^2 = \begin{pmatrix} \mathbf{m}_U^{LL2} + v_u^2 \mathbf{Y}_u \mathbf{Y}_u^\dagger & \mathbf{\Delta}^{uLR} \\ \mathbf{\Delta}^{uLR\dagger} & \mathbf{m}_U^{RR2} + v^2 \mathbf{Y}_u^\dagger \mathbf{Y}_u \end{pmatrix}, \tag{5}$$

with

$$\begin{aligned} \mathbf{\Delta}^{uLR} &= \mathbf{\Delta}^{uRL\dagger} = -v_u (\mathbf{A}_u + \mathbf{Y}_u \mu \cot\beta), \\ \mathbf{m}_U^{LL2} &= V^\dagger \mathbf{m}_Q^2 V. \end{aligned} \tag{6}$$

Here, $\mathbf{A}_u$, $\mathbf{m}_U^{LL2}$ and $\mathbf{m}_U^{RR2}$ are $3 \times 3$ matrices in flavor space and we neglected small terms involving electroweak gauge couplings; $V$ denotes the Cabibbo-Kobayashi-Maskawa (CKM) matrix. Here, we allowed for complex

Yukawa couplings and used $LR$ conventions for them and the $A$ terms [67]. Note that in Eq. (5) the Yukawa couplings and not the quark masses enter which is a relevant difference since we are computing one-loop SQCD corrections in this article.[5]

Equation (5) is given in the super-CKM basis which we define to be the basis in which the Yukawa couplings of the MSSM superpotential are diagonal, both for quarks and squarks, so that supersymmetry is manifest:

$$\mathbf{Y}_u = \begin{pmatrix} Y^{u_1} & 0 & 0 \\ 0 & Y^{u_2} & 0 \\ 0 & 0 & Y^{u_3} \end{pmatrix}. \tag{7}$$

Note that in the literature the super-CKM basis is often defined to be the basis with diagonal quark mass matrices. However, this definition has the disadvantage that the basis changes with every loop order.

We diagonalize the full Hermitian $6 \times 6$ squark mass-squared matrix $\mathcal{M}^2_{\tilde{u}}$ and the symmetric $4 \times 4$ neutralino mass matrix $\mathcal{M}_{\tilde{\chi}^0}$ as

$$W^{\tilde{u}*}_{s's} (\mathcal{M}^2_{\tilde{u}})_{s't'} W^{\tilde{u}}_{t't} = m^2_{\tilde{u}_s} \delta_{st}, \tag{8}$$

$$Z^{p'p}_N \mathcal{M}^{\tilde{\chi}_0}_{p'q'} Z^{q'q}_N = m_{\tilde{\chi}^0_p} \delta_{pq}, \tag{9}$$

where $Z_N$ and $W^{\tilde{u}}$ are unitary matrices. With these conventions we get for the squark-quark-neutralino couplings in Eq. (1)

$$\begin{aligned} \Gamma^{\tilde{\chi}^0_p L}_{\tilde{u}_s u_i} &= \frac{-e}{\sqrt{2} s_W c_W} W^{\tilde{u}*}_{is} \left( \frac{1}{3} Z^{1p}_N s_W + Z^{2p}_N c_W \right) \\ &\quad - Y^{u_i *} W^{\tilde{u}*}_{i+3,s} Z^{4p}_N, \\ \Gamma^{\tilde{\chi}^0_p R}_{\tilde{u}_s u_i} &= \frac{2\sqrt{2} e}{3 c_W} W^{\tilde{u}*}_{i+3,s} Z^{1p*}_N - Y^{u_i} W^{\tilde{u}*}_{is} Z^{4p*}_N \end{aligned} \tag{10}$$

and for the squark-quark-gluino vertex

$$\Gamma^{\tilde{g}L}_{\tilde{u}_s u_i} = -\sqrt{2} g_s T_a W^{\tilde{u}*}_{is}, \tag{11}$$

$$\Gamma^{\tilde{g}R}_{\tilde{u}_s u_i} = \sqrt{2} g_s T_a W^{\tilde{u}*}_{i+3,s}. \tag{12}$$

Here, $e$ denotes the electric charge and $s_W \equiv \sin\theta_W$, $c_W \equiv \cos\theta_W$, where $\theta_W$ is the Weinberg angle. The tree-level decay width of the lightest squark into the lightest supersymmetric particle (LSP) and a (massless) charm quark is given by

$$\Gamma_0[\tilde{u}_1 \to u_2 \tilde{\chi}^0_1] = \frac{m_{\tilde{u}_1}}{16\pi} \left( 1 - \frac{m^2_{\tilde{\chi}^0_1}}{m^2_{\tilde{u}_1}} \right)^2 \left( \left| \Gamma^{\tilde{\chi}^0_1 L}_{\tilde{u}_1 u_2} \right|^2 + \left| \Gamma^{\tilde{\chi}^0_1 R}_{\tilde{u}_1 u_2} \right|^2 \right). \tag{13}$$

If the LSP is mostly binolike, we can further simplify the expression neglecting very small neutralino mixing and small charm Yukawa couplings:

$$\Gamma_0[\tilde{u}_1 \to u_2 \tilde{\chi}^0_1] = \frac{m_{\tilde{u}_1}}{16\pi} \frac{g_1^2}{18} \left( 1 - \frac{m^2_{\tilde{\chi}^0_1}}{m^2_{\tilde{u}_1}} \right)^2 (|W^{\tilde{u}}_{21}|^2 + 16 |W^{\tilde{u}}_{51}|^2). \tag{14}$$

Note that the decay to a right-handed charm quark is enhanced by a factor 16 which can be traced back to hypercharges.

## III. CALCULATION OF THE SQCD CORRECTIONS

In this section we discuss in detail the calculation of the one-loop SQCD corrections including our renormalization scheme. Our calculation involves the following steps:

(1) Renormalization of the quark sector.
(2) Renormalization of the squark sector.
(3) Calculation of the gluon contributions to the decay width including real emission corrections, i.e. the decay $\tilde{u}_1 \to c \tilde{\chi}^0_1 g$.
(4) Calculation of the gluino contributions [including the cancellation of ultraviolet (UV) divergences].

We renormalize the fundamental parameters entering the decay width of the stop decay at tree level, which receive SQCD corrections at the one-loop level, in the dimensional reduction ($\overline{\mathrm{DR}}$) scheme. These quantities are

(i) the Yukawa couplings $Y^{u_i}$ of the MSSM superpotential,
(ii) the trilinear $A^u_{ij}$ terms, and
(iii) the bilinear squark mass terms $\mathbf{m}^{LL2}_U$ and $\mathbf{m}^{RR2}_U$.

We write the bare quantities of the Lagrangian [labeled with a superscript (0)] as

$$\begin{aligned} Y^{u_i(0)} &= Y^{u_i} + \delta Y^{u_i}, \qquad A^{u(0)}_{ij} = A^u_{ij} + \delta A^u_{ij}, \\ \mathbf{m}^{2(0)}_{Q,U} &= \mathbf{m}^2_{Q,U} + \boldsymbol{\delta}\mathbf{m}^2_{Q,U}. \end{aligned} \tag{15}$$

Since we renormalize all quantities in a minimal renormalization scheme, i.e. the $\overline{\mathrm{DR}}$ scheme, $\mathbf{A}^u$, $\mathbf{m}^2_{Q,U}$ and $\mathbf{Y}^u$ are understood to be the renormalized ones in the $\overline{\mathrm{DR}}$ scheme. However, in the decay width of the stop, the on-shell squark mass also enters. Therefore, a conversion from the on-shell squark mass to the $\overline{\mathrm{DR}}$ is necessary. In addition, the Yukawa couplings have to be related to the measured quark masses of the SM by running and threshold corrections.

[5]The threshold corrections connecting the Yukawa couplings and the quark masses are known to be very large in the down sector [68–77] and have been computed at the two-loop level [78–83].

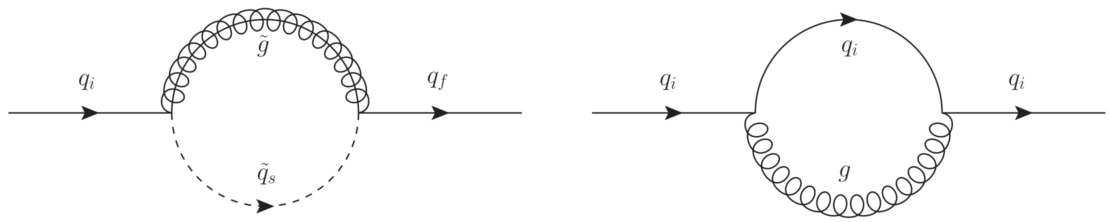


FIG. 1. Quark self-energy diagrams.

### A. Renormalization of the quark sector

SQCD corrections to quark masses and Yukawa couplings can be calculated from the quark self-energies (see Fig. 1). The UV renormalization of the Yukawa couplings (in the $\overline{\mathrm{DR}}$-bar scheme) is given by

$$\delta Y^{u_i} = -\frac{\alpha_s}{2\pi}\frac{1}{\varepsilon}C_F Y^{u_i}, \tag{16}$$

where $C_F = 4/3$ is a color factor. In our approach we compute only Lehmann-Symanzik-Zimmermann (LSZ) factors corresponding to flavor-diagonal self-energies, which are also the only UV divergent ones. All other contributions from self-energies can be calculated as one-particle irreducible diagrams [84–86]. Therefore, the LSZ factor for left- and right-handed quarks is

$$\delta Z_u^L = \delta Z_u^a + \delta Z_{u_i}^{Lb}, \tag{17}$$

$$\delta Z_u^R = \delta Z_u^a + \delta Z_{u_i}^{Rb}. \tag{18}$$

Here, the superscript $a$ denotes the flavor-independent gluon piece, while the index $b$ refers to the gluino piece whose finite part is in general flavor dependent:

$$\delta Z_u^a = \frac{\alpha_s}{4\pi}C_F(1-(1-\xi))\left[\frac{1}{\varepsilon_{\mathrm{IR}}} - \frac{1}{\varepsilon}\right], \tag{19}$$

$$\delta Z_{u_i}^{Lb} = \Sigma_{ii}^{\tilde{g}LL}, \tag{20}$$

$$\delta Z_{u_i}^{Rb} = \Sigma_{ii}^{\tilde{g}RR}. \tag{21}$$

$\xi$ denotes the gauge parameter which is involved in the gluon propagator (e.g. $\xi = 1$ would correspond to the Feynman gauge). Furthermore, $\varepsilon_{\mathrm{IR}}$ denotes the dimensionally regularized infrared (IR) divergence and $\varepsilon$ the UV one while $\Sigma_{ii}^{\tilde{g}LL}$ and $\Sigma_{ii}^{\tilde{g}RR}$ are defined in Eqs. (22) and (23).

#### *1. Threshold corrections*

In order to determine the actual values of the Yukawa couplings we have to make the connection to the quark masses determined within the SM.[6] The self-energies with heavy virtual particles, in our case the one with squarks and gluinos, lead to threshold corrections modifying the tree-level relation $v_u Y^{u_i} = m_{u_i}$. In order to write down these corrections we decompose the quark self-energies originating from squark-gluino loops as

$$\Sigma_{u_f u_i}^{\tilde{g}}(p^2) = \Sigma_{fi}^{\tilde{g}LR}(p^2)P_R + \Sigma_{fi}^{\tilde{g}RL}(p^2)P_L + \not{p}(\Sigma_{fi}^{\tilde{g}LL}(p^2)P_L + \Sigma_{fi}^{\tilde{g}RR}(p^2)P_L). \tag{22}$$

Since in the decay $\tilde{u}_1 \to c\tilde{\chi}_1^0$ we are dealing with external charm quarks on the mass shell it is sufficient to evaluate Eq. (22) at vanishing external momenta, i.e. neglecting finite terms of the order $m_c^2/m_{\mathrm{SUSY}}^2$:

$$\begin{aligned} \Sigma_{fi}^{\tilde{g}LR} &\equiv \Sigma_{fi}^{\tilde{g}LR}(0), & \Sigma_{fi}^{\tilde{g}RL} &\equiv \Sigma_{fi}^{\tilde{g}RL}(0), \\ \Sigma_{fi}^{\tilde{g}LL} &\equiv \Sigma_{fi}^{\tilde{g}LL}(0), & \Sigma_{fi}^{\tilde{g}RR} &\equiv \Sigma_{fi}^{\tilde{g}RR}(0). \end{aligned} \tag{23}$$

With these notations the relation between the Yukawa couplings of the MSSM superpotential and the running quark masses of the SM (evaluated at the scale $m_{\mathrm{SUSY}}$) is given by

$$\left[m_{u_i}\left(1 - \frac{1}{2}(\Sigma_{ii}^{\tilde{g}LL} + \Sigma_{ii}^{\tilde{g}RR})\right) - \Sigma_{ii}^{\tilde{g}LR}\right]_{\mathrm{finite}} = v_u Y^{u_i}. \tag{24}$$

### B. Renormalization of the squark sector

As for the quarks, we compute in our approach only LSZ factors corresponding to flavor-diagonal squark self-energies (i.e. $\tilde{u}_s \to \tilde{u}_s$ transitions), while all the other contributions from squark self-energies are calculated as one-particle irreducible diagrams. The LSZ factors for the squarks then read

$$\delta\tilde{Z}_{\tilde{u}}^a = \frac{\alpha_s}{4\pi}C_F(2+(1-\xi))\left[\frac{1}{\varepsilon} - \frac{1}{\varepsilon_{\mathrm{IR}}}\right], \tag{25}$$

$$\delta\tilde{Z}_{\tilde{u}_s}^b = \left.\frac{\partial\Sigma_{\tilde{u}_s\tilde{u}_s}^{\tilde{g}+\tilde{q}}(p^2)}{\partial p^2}\right|_{p^2=m_{\tilde{u}_s}^2} = -\frac{\alpha_s}{2\pi}C_F\frac{1}{\varepsilon} + \text{finite}. \tag{26}$$

Like in the quark case $a$ refers to the gluon part and $b$ to the gluino and squark-tadpole part and $\Sigma_{\tilde{u}_s\tilde{u}_s}^{\tilde{g}+\tilde{q}}(p^2)$ denotes the sum of Eqs. (A19) and (A24). From Eqs. (A19)–(A24) in the Appendix we find that the sum of those UV divergent parts of the squark self-energies which are independent of the external momentum (i.e. the masslike contribution) is given by

[6] For a complete discussion of all one-loop corrections within the MSSM including resummation see Ref. [67].

$$\Sigma^{\mathrm{UVdiv}}_{\tilde{u}_s\tilde{u}_t}(0) = \frac{\alpha_s}{2\pi}C_F\frac{1}{\varepsilon}\Bigg[\left(\frac{\xi-1}{2}m^2_{\tilde{u}_s}+m^2_{\tilde{g}}\right)\delta_{st}+2\sum_{j=1}^{3}(W^{\tilde{u}*}_{js}m^2_{u_j}W^{\tilde{u}}_{jt}+W^{\tilde{u}*}_{j+3,s}m^2_{u_j}W^{\tilde{u}}_{j+3,t})$$
$$+\sum_{i,j=1}^{3}(W^{\tilde{u}\star}_{i+3s}\Delta^{uRL}_{ij}W^{\tilde{u}}_{jt}+W^{\tilde{u}\star}_{is}\Delta^{uLR}_{ij}W^{\tilde{u}}_{j+3t})-2m_{\tilde{g}}\sum_{j=1}^{3}(W^{\tilde{u}*}_{js}m_{u_j}W^{\tilde{u}}_{j+3,t}+W^{\tilde{u}*}_{j+3,s}m_{u_j}W^{\tilde{u}}_{jt})\Bigg]. \tag{27}$$

Here, $m_{\tilde{g}}$ denotes the gluino mass. To Eq. (27), the divergent squark mass terms induced by the LSZ factors in Eqs. (25) and (26)

$$\frac{\alpha_s}{4\pi}C_F(1-\xi)\frac{1}{\varepsilon}m^2_{\tilde{u}_s}\delta_{st} \tag{28}$$

have to be added, canceling the divergence involving $m^2_{\tilde{u}_s}$. In order to see the cancellation of the remaining UV divergences in Eq. (27), we consider the bare mass matrix which is given in the super-CKM basis

$$\mathcal{M}^{2(0)}_{\tilde{u}} = \begin{pmatrix} m^{LL2}_U+\delta m^{LL2}_U+v_u^2(Y^u\delta Y^{u\dagger}+\delta Y^uY^{u\dagger}) & -v_u(A^u+\delta A^u+\mu(Y^u+\delta Y^u)\cot\beta) \\ -v_u(A^{u\dagger}+\delta A^{u\dagger}+\mu(Y^{u\dagger}+\delta Y^{u\dagger})\cot\beta) & m^{RR2}_U+\delta m^{RR2}_U+v_u^2(Y^u\delta Y^{u\dagger}+\delta Y^uY^{u\dagger}) \end{pmatrix}. \tag{29}$$

Since the squark-mixing matrix $W^{\tilde{u}}$ diagonalizes the renormalized mass matrix, the bare mass matrix is not diagonal in this basis but rather has the form

$$W^{\tilde{u}*}_{s's}(\mathcal{M}^{2(0)}_{\tilde{u}})_{s't'}W^{\tilde{u}}_{t't} = m^2_{\tilde{u}_s}\delta_{st}+\sum_{i,j=1}^{3}[v_u^2(W^{\tilde{u}*}_{is}(Y^u\delta Y^{u\dagger}+\delta Y^uY^{u\dagger})_{ij}W^{\tilde{u}}_{jt}$$
$$+W^{\tilde{u}*}_{i+3,s}(Y^u\delta Y^{u\dagger}+\delta Y^uY^{u\dagger})_{ij}W^{\tilde{u}}_{j+3,t})+W^{\tilde{u}*}_{is}\delta m^{LL2}_{Uij}W^{\tilde{u}}_{jt}+W^{\tilde{u}*}_{i+3,s}\delta m^{RR2}_{Uij}W^{\tilde{u}}_{j+3,t})$$
$$-v_u(W^{\tilde{u}\star}_{i+3s}(\delta A^{u\dagger}+\mu\delta Y^{u\dagger}\cot\beta)_{ij}W^{\tilde{u}}_{jt}+W^{\tilde{u}\star}_{is}(\delta A^u+\mu\delta Y^u\cot\beta)_{ij}W^{\tilde{u}}_{j+3t})]. \tag{30}$$

Comparing Eqs. (27) and (28) to Eq. (30), we observe that the counterterms

$$v_u\delta Y^{u_i} = -\frac{\alpha_s}{2\pi}\frac{1}{\varepsilon}C_Fm_{u_i} \tag{31}$$

and

$$\delta A^u_{ij} = -\frac{\alpha_s}{2\pi}\frac{1}{\varepsilon}C_F(A^u_{ij}+2m_{\tilde{g}}Y^{u_i}\delta_{ij}), \tag{32}$$

$$(\delta m^{LL2}_U)_{ij} = (\delta m^{RR2}_U)_{ij} = -\frac{\alpha_s}{2\pi}\frac{1}{\varepsilon}C_Fm^2_{\tilde{g}}\delta_{ij} \tag{33}$$

cancel the divergences. As required by supersymmetry, Eq. (31) equals Eq. (16). Therefore, no renormalization of the squark-mixing matrices $W$ is necessary in this formalism.[7]

In the numerical analysis, we will use the connection between the on-shell and the $\overline{\mathrm{DR}}$ mass. This relation is given by

$$m^{2\,\mathrm{OS}}_{\tilde{u}_s} = m^{2\,\overline{\mathrm{DR}}}_{\tilde{u}_s}+\Sigma^{\mathrm{finite}}_{\tilde{u}_s\tilde{u}_s}(p^2=m^2_{\tilde{u}_s}). \tag{34}$$

### C. Gluon contributions

Here, we combine the virtual gluon contributions with the real radiation (see Fig. 2) and show the cancellation of the infrared and collinear divergences. In our calculations all singularities are regularized dimensionally; more precisely, we use dimensional reduction and introduce the renormalization scale in the form $\mu^2e^\gamma/(4\pi)$, where $\gamma = 0.577\ldots$ is the Euler constant.

For the vertex correction diagram due to gluon exchange (left diagram in Fig. 3) we get

$$V^g = \mathcal{A}_0\frac{\alpha_s}{4\pi}C_F\Bigg[\frac{(1-(1-\xi))}{\varepsilon}-\frac{1}{\varepsilon^2_{\mathrm{IR}}}+\frac{-2+(1-\xi)-2L_\mu+2\ln(1-x_1)}{\varepsilon_{\mathrm{IR}}}-2-\frac{\pi^2}{12}$$
$$-2L_\mu^2-2L_\mu+4L_\mu\ln(1-x_1)-2\ln^2(1-x_1)+2\ln(1-x_1)-2\mathrm{Li}_2(x_1)\Bigg], \tag{35}$$

[7]Furthermore, note that since the renormalization of the Yukawa couplings is fixed from the quark sector to be in a minimal renormalization scheme, it would not be consistent to absorb the finite pieces of the loop corrections into a redefinition of the squark-mixing matrices.

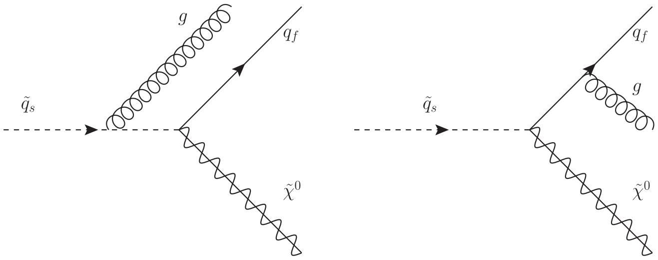

FIG. 2. Feynman diagrams showing the real emission of a gluon, i.e. the process $\tilde{u}_1 \to c + g + \tilde{\chi}_1^0$.

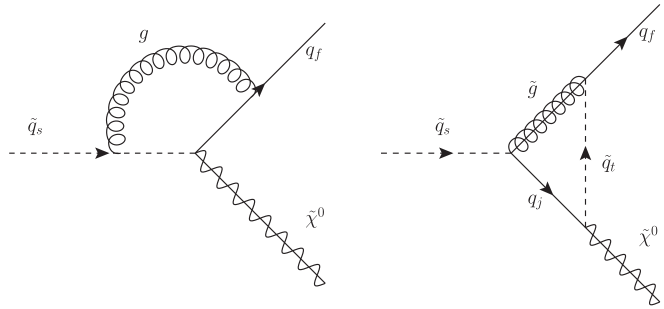

FIG. 3. Genuine vertex corrections involving gluons (left diagram) and gluinos (right diagram).

using the abbreviations $x_1 = m^2_{\tilde{\chi}_1^0}/m^2_{\tilde{u}_1}$ and $L_\mu = \ln(\mu/m_{\tilde{u}_1})$. $\xi$ denotes the gauge parameter which is involved in the gluon propagator. As before, poles of the form $1/\varepsilon$ correspond to ultraviolet singularities, while poles of the form $1/\varepsilon_{\rm IR}^2$, $1/\varepsilon_{\rm IR}$ are due to infrared and collinear singularities. Finally $\mathcal{A}_0$ is the tree-level amplitude [originating from Eq. (1)], reading

$$\mathcal{A}_0 = i\bar{u}(p_{u_2})\Big(\Gamma^{\tilde{\chi}_1^0 L\star}_{\tilde{u}_1 u_2} P_R + \Gamma^{\tilde{\chi}_1^0 R\star}_{\tilde{u}_1 u_2} P_L\Big) v(p_{\tilde{\chi}_1^0}). \qquad (36)$$

To get the renormalized result $\mathcal{A}^g$ for the amplitude, we need to add the contributions induced by the gluon part of the LSZ factors of the (massless) charm quark and the stop squark [see Eqs. (19) and (25), respectively], as well as the effects induced by the renormalization constants for the coupling constants $e$ and $Y^{u_i}$ appearing in the tree-level squark-quark-neutralino vertex. These renormalization constants are written as $Z_e = 1 + \delta Z_e^a + \delta Z_e^b$ for the gauge coupling $e$ and $Z_{Y^{u_i}} = 1 + \delta Z^a_{Y^{u_i}} + \delta Z^b_{Y^{u_i}}$ for the Yukawa coupling $Y^{u_i}$. The parts due to gluon corrections, which are relevant in this subsection, read[8]

$$\delta Z_e^a = \delta Z^a_{Y^{u_i}} = -\frac{\alpha_s}{4\pi} C_F \frac{3}{2}\frac{1}{\varepsilon}. \qquad (37)$$

As expected, these expressions are independent of the gauge parameter $\xi$. Adding up the mentioned contributions, we get the renormalized amplitude

$$\begin{aligned}\mathcal{A}^g = \mathcal{A}_0 \frac{\alpha_s}{4\pi} C_F \Big[ &-\frac{1}{\varepsilon_{\rm IR}^2} + \frac{-5/2 - 2L_\mu + 2\ln(1-x_1)}{\varepsilon_{\rm IR}} - 2 - \frac{\pi^2}{12} \\ &-2L_\mu^2 - 2L_\mu + 4L_\mu \ln(1-x_1) - 2\ln^2(1-x_1) + 2\ln(1-x_1) - 2{\rm Li}_2(x_1)\Big]. \end{aligned} \qquad (38)$$

This result is, as required by consistency, again independent of the gauge parameter $\xi$. After squaring the renormalized amplitude and performing the phase-space integrals (working consistently in $d = 4 - 2\varepsilon$ dimensions), we get the decay width

$$\begin{aligned}\Gamma^{\rm virt} = \Gamma_0 \frac{\alpha_s}{4\pi} C_F \Big[ &-\frac{2}{\varepsilon_{\rm IR}^2} + \frac{-9 - 8L_\mu + 8\ln(1-x_1)}{\varepsilon_{\rm IR}} - 22 + \frac{\pi^2}{3} - 16L_\mu^2 \\ &- 30L_\mu + 32L_\mu \ln(1-x_1) - 16\ln^2(1-x_1) + 30\ln(1-x_1) - 4{\rm Li}_2(x_1)\Big], \end{aligned} \qquad (39)$$

where $\Gamma_0$ is the corresponding decay width at order $\alpha_s^0$ given in Eq. (13).

We now turn to the bremsstrahlung corrections (see Fig. 2). Using the information given in Section A 1 of the Appendix on the three-particle phase space and making use of the mathematica package HypExp 2.0 [87], it is straightforward to derive the decay width for $\tilde{u}_1 \to c\tilde{\chi}_1^0 g$. We obtain

[8]The parts $\delta Z_e^b$ and $\delta Z^b_{Y^{u_i}}$, which are due to gluino corrections, will be taken into account in the following subsection.

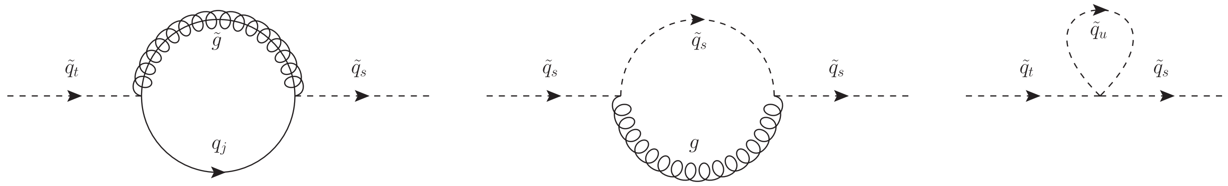


FIG. 4. Squark self-energy diagrams with SQCD loops: Gluon, gluino and tadpole contribution (from left to right).

$$\Gamma^{\rm brems} = \Gamma_0 \frac{\alpha_s}{4\pi} C_F \bigg[\frac{2}{\varepsilon_{\rm IR}^2} + \frac{9+8L_\mu - 8\ln(1-x_1)}{\varepsilon_{\rm IR}} - \frac{5\pi^2}{3} + \frac{69-71x_1}{2(1-x_1)} + 16L_\mu^2 + 36L_\mu \\ - 32L_\mu \ln(1-x_1) + 16\ln^2(1-x_1) - 4(9+\ln(x_1))\ln(1-x_1) - \frac{x_1(4-3x_1)}{(1-x_1)^2}\ln(x_1) - 4{\rm Li}_2(x_1)\bigg]. \tag{40}$$

Adding the virtual corrections (39) and the gluon bremsstrahlung corrections (40), we get

$$\Gamma^g = \Gamma_0 \frac{\alpha_s}{4\pi} C_F \bigg[-\frac{4\pi^2}{3} + \frac{25-27x_1}{2(1-x_1)} + 6L_\mu - 2(3+2\ln(x_1))\ln(1-x_1) - \frac{x_1(4-3x_1)}{(1-x_1)^2}\ln(x_1) - 8{\rm Li}_2(x_1)\bigg]. \tag{41}$$

As expected, the collinear and infrared singularities canceled and the result is finite.[9]

### D. Gluino and squark-tadpole contributions

We write the amplitude containing the tree level and the contribution of loop diagrams involving gluinos and the squark tadpole (right diagram in Fig. 4) as

$$\mathcal{A}^{\tilde{g}} = i\bar{u}(p_{u_2})\bigg[\bigg(\Gamma^{\tilde{\chi}_1^0 L*}_{\tilde{u}_1 u_2} + \Lambda^{\tilde{\chi}_1^0 L*}_{\tilde{u}_1 u_2} + \sum_{j=1}^{3} X^{L*}_{u_j u_2}\Gamma^{\tilde{\chi}_a^0 L*}_{\tilde{u}_1 u_j} + \sum_{s=1}^{6}\Gamma^{\tilde{\chi}_1^0 L*}_{\tilde{u}_s u_2}\tilde{X}_{\tilde{u}_s \tilde{u}_1}\bigg)P_R + (R\leftrightarrow L)\bigg]v(p_{\tilde{\chi}_1^0}). \tag{42}$$

Here, $\Gamma^{\tilde{\chi}_1^0 L*}_{\tilde{u}_1 u_2}$ encodes the tree-level contribution and $\Lambda^{\tilde{\chi}_1^{0*}}_{\tilde{u}_1 u_2}$, given in Eq. (A9) of the Appendix, denotes the genuine vertex correction involving the gluino. Furthermore, $X^{L,R}_{u_f u_i}$ and $\tilde{X}_{\tilde{u}_s \tilde{u}_t}$ originate from quark and squark self-energy diagrams, respectively. The explicit expressions read

$$\tilde{X}_{\tilde{u}_s \tilde{u}_t} = \begin{cases} \frac{\Sigma_{\tilde{u}_s \tilde{u}_t}(p^2 = m^2_{\tilde{u}_t})}{m^2_{\tilde{u}_t} - m^2_{\tilde{u}_s}} & \text{for } s \neq t, \\ \frac{1}{2}\delta\tilde{Z}^b_{\tilde{u}_s} & \text{for } s = t, \end{cases} \tag{43}$$

$$X^L_{u_f u_i} = \begin{cases} \frac{m_i \Sigma^{\tilde{g}LR}_{fi} + m_f \Sigma^{\tilde{g}RL}_{fi} + m_i^2 \Sigma^{\tilde{g}LL}_{fi} + m_f m_i \Sigma^{\tilde{g}RR}_{fi}}{m_i^2 - m_f^2} & \text{for } f \neq i, \\ \frac{1}{2}\delta Z^{Lb}_{u_f} & \text{for } f = i. \end{cases} \tag{44}$$

Let us briefly discuss the ultraviolet singularities in Eq. (42) and how they get canceled: All divergences in the off-diagonal elements of $\tilde{X}_{\tilde{u}_s \tilde{u}_t}$ are canceled by the counterterms induced through the renormalization of $Y^{u_i}, A^u_{ij}, (m^{LL2}_U)_{ij}$ and $(m^{RR2}_U)_{ij}$ in the squark mass matrix, while the off-diagonal elements of $X^{L,R}_{u_f u_i}$ are finite *ab initio*. Therefore, we are effectively left in Eq. (42) with the singularities in the flavor conserving parts of $X^{L,R}_{u_f u_i}$ and $\tilde{X}_{\tilde{u}_s \tilde{u}_t}$ which originate from LSZ factors, and with the singularities present in the vertex correction $\Lambda^{\tilde{\chi}_1^0 L*}_{\tilde{u}_1 u_2}$. Using the unitarity of the squark-mixing matrices in Eq. (A9), the latter singularities read

$$\Lambda^{\tilde{\chi}_1^0 L*}_{\tilde{u}_1 u_2;{\rm div}} = \frac{-\alpha_s}{2\pi} C_F \frac{1}{\varepsilon} W^{\tilde{u}}_{2+3,1} Y^{u_2} Z_N^{41*}, \\ \Lambda^{\tilde{\chi}_1^0 R*}_{\tilde{u}_1 u_2;{\rm div}} = \frac{-\alpha_s}{2\pi} C_F \frac{1}{\varepsilon} W^{\tilde{u}}_{2,1} Y^{u_2 *} Z_N^{41}. \tag{45}$$

[9] As the renormalization scheme in Ref. [66] is quite different from ours, a full comparison is difficult. It was, however, possible to compare the gluino vertex correction, the virtual gluon corrections and the gluon bremsstrahlung corrections individually. Taking into account that in Ref. [66] the two-particle phase space (and a corresponding part of the three-particle phase space) is in $d = 4$ dimensions and that the renormalization scale is of the form $\mu^{2\varepsilon}\Gamma(1-\varepsilon)/(4\pi)^\varepsilon$, we found that the results are in agreement. In our calculation we used a $d$-dimensional phase space [and introduce the renormalization scale in the form $\mu^{2\varepsilon}e^{\gamma\varepsilon}/(4\pi)^\varepsilon$].

It is straightforward to see that the remaining singularities get canceled against those which are induced by the gluino parts $\delta Z_e^b$ and $\delta Z_{Y^{u_i}}^b$ of the renormalization constants of the gauge coupling $e$ and $Y^{u_i}$ present in the tree-level squark-quark-neutralino vertex. These renormalization constants read[10]

$$\delta Z_e^b = -\delta Z_e^a, \tag{46}$$

$$\delta Z_{Y^{u_i}}^b = -\frac{\alpha_s}{8\pi} C_F \frac{1}{\varepsilon}, \tag{47}$$

where $Z_e^a$ is given in Eq. (37).

Therefore, the renormalized version of the amplitude is obtained by just taking the finite part of Eq. (42). The corresponding contribution to the decay width is then obtained by inserting the renormalized amplitude into Eq. (13) and working out the interference term, i.e. the term proportional to $\alpha_s$.

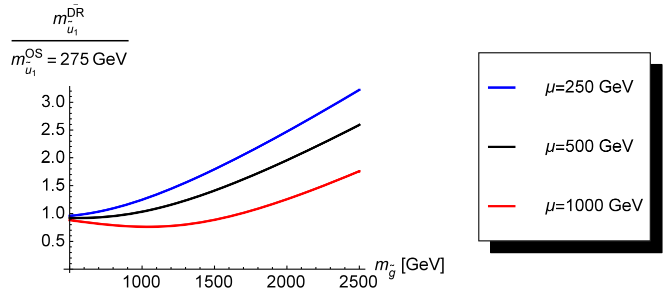


FIG. 5 (color online). Ratio of the $\overline{\rm DR}$ stop mass over its on-shell mass for $m_{\tilde{u}_1}^{\rm OS} = 275$ GeV as generated by Eq. (48) and $A^t = 1$ TeV as a function of the gluino mass for different values of the renormalization scale $\mu$ (see text).

## IV. NUMERICAL ANALYSIS

In our numerical analysis we investigate the size of the calculated SQCD corrections. For this purpose we consider the following squark mass matrix given in the $\overline{\rm DR}$ scheme:

$$\mathcal{M}_{\tilde{u}}^2 = \begin{pmatrix} (2\ \text{TeV})^2 & 0 & 0 & 0 & 0 & 0 \\ 0 & (2\ \text{TeV})^2 & \Delta_{23}^{LL} & 0 & 0 & \Delta_{23}^{LR} \\ 0 & \Delta_{23}^{LL*} & (m_{33}^{LL})^2 & 0 & \Delta_{23}^{RL*} & -v_u A^t \\ 0 & 0 & 0 & (2\ \text{TeV})^2 & 0 & 0 \\ 0 & 0 & \Delta_{23}^{RL} & 0 & (2\ \text{TeV})^2 & \Delta_{23}^{RR} \\ 0 & \Delta_{23}^{LR*} & -v_u A^t & 0 & \Delta_{23}^{RR*} & (m_{33}^{RR})^2 \end{pmatrix}. \tag{48}$$

Here, $\Delta_{ij} = \delta_{ij}\sqrt{\mathcal{M}_{\tilde{u},ii}^2 \mathcal{M}_{\tilde{u},jj}^2}$ parametrizes the flavor change (and is assumed to be small compared to the diagonal elements) and we choose $A^t = \pm 1$ TeV. In the following, we will consider the case of $m_{33}^{RR} = m_{33}^{LL}$ (i.e. maximal mixing). For the neutralino, which we assume to be binolike, we choose a mass of 250 GeV and use $\alpha_s(m_{\rm SUSY}) = 0.087$ as an input.

At tree level, the scheme for the stop mass is not defined. At the one-loop level the quantities of the MSSM superpotential must be renormalized in a process-independent way in order to respect supersymmetry; e.g. the Yukawa couplings have to be renormalized in the $\overline{\rm DR}$ scheme. For consistency, also all other elements of the squark mass matrix should be renormalized in this scheme as well and should be given at the same renormalization scale. After diagonalization of the squark mass matrix, the eigenvalues correspond to $\overline{\rm DR}$ masses which can be translated to on-shell masses if necessary or desired. This is the case for $\tilde{u}_1 \to c\tilde{\chi}_1^0$ where the masses entering the decay width in Eq. (13) are on-shell masses.

The shift between the $\overline{\rm DR}$ and the on-shell mass [see Eq. (34)] turns out to be numerically especially important for our scenario with a light stop because it scales like[11] $m_{\tilde{g}}^2/m_{\tilde{q}}^2$. In Fig. 5 we show the ratio $m_{\tilde{u}_1}^{\overline{\rm DR}}/m_{\tilde{u}_1}^{\rm OS}$ as a function of the gluino mass at the one-loop level for $m_{\tilde{u}_1}^{\rm OS} = 275$ GeV. For this we set all flavor off-diagonal elements $\Delta_{ij}$ in Eq. (48) to zero.

Note that for large gluino masses the on-shell stop mass is smaller than the $\overline{\rm DR}$ mass. This has interesting consequences for model building with light stops: Assuming that there is already a splitting between the $\overline{\rm DR}$ squark masses of the first two generations and the stop squark (for example due to the running from the GUT scale to the SUSY scale) at the SUSY scale, then this splitting is significantly increased for heavy gluinos, making the stop even lighter. Therefore, light stop

[10] $\delta Z_e^b = -\delta Z_e^b$ verifies that the electric charge is not renormalized by SQCD and the compatibility of $\delta Z_{Y^{u_i}}^a + \delta Z_{Y^{u_i}}^b$ with Eq. (16) shows that SUSY is respected.

[11] Even though the correction is very large, perturbation theory still works, because the parametric enhancement $m_{\tilde{g}}^2/m_{\tilde{q}}^2$ can only appear once at any loop level. Therefore, higher loop corrections will have the size of ordinary SQCD effects compared to the one-loop result. The relation is known at the two-loop level [88].

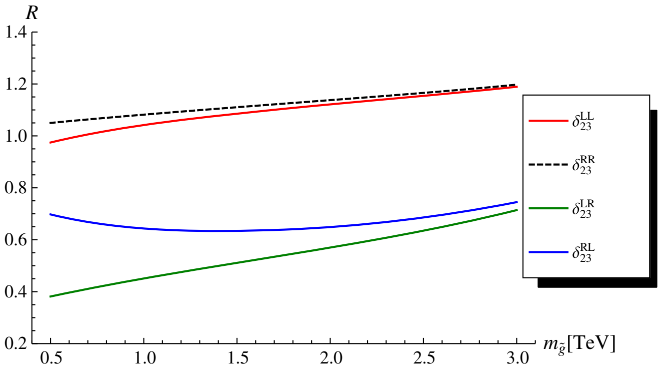


FIG. 6 (color online). Ratio of the decay width including the one-loop SQCD corrections over the tree-level decay width for different sources of flavor violation as a function of the gluino mass for $A^t = 1$ TeV. The renormalization scale is chosen to be $\mu = 275$ GeV.

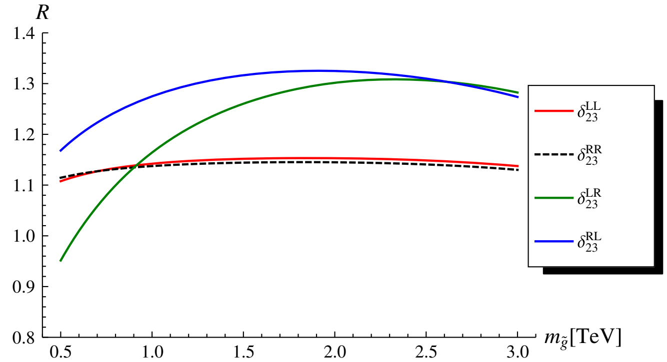


FIG. 7 (color online). Ratio of the decay width including the one-loop SQCD corrections over the tree-level decay width for different sources of flavor violation as a function of the gluino mass for $A^t = -1$ TeV. The renormalization scale is chosen to be $\mu = 275$ GeV.

scenarios, which are interesting for the decay $\tilde{u}_1 \to c\tilde{\chi}_1^0$, can be even generated via finite loop effects.

For the numerical analysis of the SQCD corrections to $\tilde{u}_1 \to c\tilde{\chi}_1^0$, we choose $m_{33}^{LL} = m_{33}^{RR}$ in Eq. (48) in such a way, that a given on-shell mass for $\tilde{u}_1$ (275 GeV in our example) results after diagonalizing Eq. (48) and shifting the so-obtained $\overline{\mathrm{DR}}$ squark masses to the corresponding on-shell masses.[12] This procedure we do for both the tree-level decay width $\Gamma^{\mathrm{tree}}$ and for the SQCD corrected version $\Gamma^{\mathrm{one\text{-}loop}}$ calculated in this paper.

In Fig. 6 (Fig. 7) we illustrate the effect of the one-loop contributions for positive (negative) $A^t$ for the four different sources of flavor violation: $\delta_{23}^{RR}$, $\delta_{23}^{LL}$, $\delta_{23}^{RL}$ and $\delta_{23}^{LR}$. Here, we defined the ratio $R = \Gamma^{\mathrm{one\text{-}loop}}/\Gamma^{\mathrm{tree}}$ of the partial widths. In each of the four curves in Figs. 6 and 7 the indicated $\delta_{ij}^{AB}$ is put to 0.01, while the other $\delta$'s are switched off. Note that the actual numerical values of the mentioned $\delta$'s drop out in this ratio to a very good approximation. We find that if bilinear terms are the only sources of flavor violation, the SQCD effects are around 10%, while if flavor violations originate from trilinear terms the corrections can reach ±50% or even more. The large corrections in the case of $\delta_{23}^{RL}$ and $\delta_{23}^{LR}$ can be traced back to the suppressed decay width for left-handed charm quarks.

As stated above, we renormalize all quantities in a minimal renormalization scheme, i.e. in the $\overline{\mathrm{DR}}$ scheme, and relate the Yukawa couplings to the ones obtained within the SM by running and threshold corrections. Reference [66] used an on-shell renormalization scheme in which the counterterms to the quark- and squark-mixing matrices are fixed in such a way that they exactly cancel the anti-Hermitian parts of the LSZ factors of the quarks and the squarks. While to all orders in perturbation theory the final result must of course be independent of the renormalization scheme, at a finite loop order, different schemes have (dis)advantages compared to each other. A minimal renormalization scheme is process independent and allows combining different quantities (like for example those appearing in the squark mass matrix) if they are given at the same renormalization scale. Furthermore, if one aims at studying the consequences of a model with high-scale SUSY breaking, a minimal renormalization scheme is preferred since running quantities are involved so that the different scales can be connected. Furthermore, when using a mixed on-shell $\overline{\mathrm{DR}}$ scheme, one must be careful not to renormalize dependent quantities (connected by SUSY relations) entering at various places in a different way. For example, renormalizing the squark-mixing matrices on shell might be in conflict with the $\overline{\mathrm{DR}}$ renormalization of the Yukawa couplings within the squark mass matrices, entering the determination of $W^{\tilde{u}}$.

## V. CONCLUSIONS

In this article we computed the one-loop SQCD corrections to the decay $\tilde{u}_1 \to c\tilde{\chi}_1^0$ in the MSSM with generic sources of flavor violation. This decay is phenomenologically very important if the mass splitting between the neutralino and the lightest stop is smaller than the top mass. In particular, we pointed out that a sizable partial width for $\tilde{u}_1 \to c\tilde{\chi}_1^0$, which is possible in the presence of nonminimal sources of flavor violation, can significantly weaken the LHC exclusion bounds obtained from $\tilde{u}_1 \to Wb\chi_1^0$ where usually a branching ratio of 100% is assumed.

Working in the super-CKM basis with diagonal Yukawa couplings and renormalizing all parameters in the $\overline{\mathrm{DR}}$ scheme, we explicitly checked for the cancellation of UV divergences and verified that SUSY relations are satisfied. In particular, in the squark sector all divergences are eliminated by flavor-conserving counterterms to Yukawa couplings, $A$ terms and the bilinear terms, meaning

[12] $m_{33}^{LL} = m_{33}^{RR}$ determined in this way will depend on the gluino mass $m_{\tilde{g}}$ and on the renormalization scale $\mu$.

that no renormalization of the squark-mixing matrices is necessary. Concerning the gluon corrections we regularized all divergences dimensionally and verified their cancellation in a general $R_\xi$ gauge.

Numerically, we observe a large shift between the on-shell and the $\overline{\mathrm{DR}}$ mass of the stop. Due to the inherited quadratic divergence, the shift involves a term proportional to $m_{\tilde{g}}^2/m_{\tilde{q}}^2$. Since for large gluino masses the on-shell stop mass is driven to smaller values compared to the $\overline{\mathrm{DR}}$ mass, it is important to take into account this shift for model building. Taking the on-shell stop mass as an input, we find a SQCD enhancement of the decay width compared to the tree level for $\tilde{u}_1 \to c\tilde{\chi}_1^0$ (assuming a binolike LSP) of approximately 10% if the flavor violation is due to bilinear terms and ±50% and more if the single origin of flavor violation is the trilinear terms.

For the future, a NLO SQCD calculation of $\tilde{u}_1 \to Wb\chi_1^0$ would be desirable and a phenomenological study of the impact of $\tilde{u}_1 \to c\tilde{\chi}_1^0$ on the exclusion bounds from $\tilde{u}_1 \to Wb\chi_1^0$ is planned.

## ACKNOWLEDGMENTS

This work is supported by the Swiss National Science Foundation. A. C. is supported by a Marie Curie Intra-European Fellowship of the European Community's 7th Framework Programme under Contract No. (PIEF-GA-2012-326948). We would like to thank the authors of Ref. [66] for their kind help in comparing the details of the real emission part and for useful comments on the manuscript.

## APPENDIX

### 1. Relevant phase-space formulas

The fully differential decay width $d\Gamma$ for a generic process $p \to p_1 + p_2 + \cdots + p_n$ can be written as

$$d\Gamma = \frac{1}{2m}\overline{|M|^2} D\Phi(1 \to n), \tag{A1}$$

where $\overline{|M|^2}$ is the squared matrix element, summed and averaged over spins and colors of the particles in the final and initial state, respectively, and $m$ is the mass of the decaying particle.

In Refs. [89,90] useful parametrizations for the phase-space factors $D\Phi(1 \to n)$ have been given for $n = 3, 4$, for the case where all final-state particles are massive. In our problem we only use the case $n = 3$ where only the neutralino is massive; this means that the general formula simplifies. In the following subsection we see that the three-particle phase space can be parametrized in terms of two parameters $\lambda_1$ and $\lambda_2$, which run independently in the range [0, 1]. Of course, all scalar products involved in $|M|^2$ can be expressed in terms of these parameters.

#### a. Phase-space parametrization for the three-particle final state

In our application we identify $p_1$ with the neutralino, $p_2$ with the (massless) charm quark and $p_3$ with the gluon and define $x_1 = m_{\tilde{\chi}_1^0}^2/m_{\tilde{u}_1}^2$. Starting from Eq. (2.10) of Ref. [89], one gets

$$\begin{aligned} D\Phi(1 \to 3) = {} & \frac{m_{\tilde{u}_1}^{2d-6} 2^{1-2d} \pi^{1-d}}{\Gamma(d-2)} [(1-\lambda_1)\lambda_1]^{\frac{d-4}{2}} [(1-\lambda_2)\lambda_2]^{d-3} \\ & \times (1-x_1)^{2d-5} [\lambda_2(1-x_1) + x_1]^{\frac{2-d}{2}} d\lambda_1 d\lambda_2. \end{aligned} \tag{A2}$$

The scalar products of the momenta $p_i$, encoded in the quantities $s_{ij} = (p_i + p_j)^2/m_{\tilde{u}_1}^2$, can be written in terms of the parameters $\lambda_1$ and $\lambda_2$ as

$$\begin{aligned} s_{13} &= \lambda_2(1-x_1) + x_1 \\ s_{12} &= \frac{\lambda_1(\lambda_2-1)\lambda_2(1-x_1)^2 - x_1}{\lambda_2(x_1-1) - x_1}. \end{aligned}$$

### 2. Loop functions

The one-loop functions which appear at various places in this Appendix are defined as

$$A_0(m^2) = \frac{16\pi^2}{i}\frac{\mu^{2\epsilon}e^{\gamma\epsilon}}{(4\pi)^\epsilon}\int \frac{d^d\ell}{(2\pi)^d}\frac{1}{[\ell^2 - m^2]} \tag{A3}$$

$$\begin{aligned} B_0(p^2; m_1^2, m_2^2) &= \frac{16\pi^2}{i}\frac{\mu^{2\epsilon}e^{\gamma\epsilon}}{(4\pi)^\epsilon} \\ &\quad \times \int \frac{d^d\ell}{(2\pi)^d}\frac{1}{[\ell^2 - m_1^2][(\ell+p)^2 - m_2^2]} \\ &= \mu^{2\epsilon}e^{\gamma\epsilon}\Gamma(\epsilon) \\ &\quad \times \int_0^1 [-x(m_1^2 - m_2^2 + p^2) + m_1^2 + p^2x^2]^{-\epsilon} \end{aligned} \tag{A4}$$

$$\begin{aligned} B_1(p^2; m_1^2, m_2^2)p^\mu &= \frac{16\pi^2}{i}\frac{\mu^{2\epsilon}e^{\gamma\epsilon}}{(4\pi)^\epsilon}\int \frac{d^d\ell}{(2\pi)^d}\frac{\ell^\mu}{[\ell^2 - m_1^2][(\ell+p)^2 - m_2^2]} \\ &= p^\mu \frac{A_0(m_1^2) - A_0(m_2^2) - (p^2 + m_1^2 - m_2^2)B_0(p^2; m_1^2, m_2^2)}{2p^2} \end{aligned} \tag{A5}$$

$$B_2(p^2;m_1^2,m_2^2)=\frac{16\pi^2}{i}\frac{\mu^{2\varepsilon}e^{\gamma\varepsilon}}{(4\pi)^\varepsilon}\int\frac{d^d\ell}{(2\pi)^d}\frac{\ell^2}{[\ell^2-m_1^2][(\ell+p)^2-m_2^2]}=A_0(m_2^2)+m_1^2B_0(p^2;m_1^2,m_2^2) \tag{A6}$$

$$\begin{aligned}C_0(p_1^2,(p_1-p_2)^2,p_2^2;m_0^2,m_1^2,m_2^2)&=\frac{16\pi^2}{i}\frac{\mu^{2\varepsilon}e^{\gamma\varepsilon}}{(4\pi)^\varepsilon}\int\frac{d^d\ell}{(2\pi)^d}\frac{1}{[\ell^2-m_0^2][(\ell+p_1)^2-m_1^2][(\ell+p_2)^2-m_2^2]}\\&=-\mu^{2\varepsilon}e^{\gamma\varepsilon}\Gamma(\varepsilon+1)\int_0^1dx\int_0^{1-x}dy[-x(m_0^2-m_1^2+p_1^2)\\&\quad-y(m_0^2-m_2^2+p_2^2)+m_0^2+p_1^2x^2+2xyp_1\cdot p_2+p_2^2y^2]^{-(1+\varepsilon)}\end{aligned} \tag{A7}$$

$$\begin{aligned}C_2(p_1^2,(p_1-p_2)^2,p_2^2;m_0^2,m_1^2,m_2^2)&=\frac{16\pi^2}{i}\frac{\mu^{2\varepsilon}e^{\gamma\varepsilon}}{(4\pi)^\varepsilon}\int\frac{d^d\ell}{(2\pi)^d}\frac{\ell^2}{[\ell^2-m_0^2][(\ell+p_1)^2-m_1^2][(\ell+p_2)^2-m_2^2]}\\&=B_0((p_2-p_1)^2;m_1^2,m_2^2)+m_0^2C_0(p_1^2,(p_1-p_2)^2,p_2^2;m_0^2,m_1^2,m_2^2).\end{aligned} \tag{A8}$$

### 3. Vertex correction involving the gluino

The correction of the squark-quark-neutralino vertex involving the gluino (see the right frame of Fig. 3) reads

$$\begin{aligned}\Lambda^{\tilde\chi_1^0*}_{\tilde u_1u_2}=\frac{-1}{16\pi^2}\sum_{j,s}\Big[\Gamma^{\tilde gL*}_{\tilde u_su_2}\Big(&C_2\Gamma^{\tilde gR*}_{\tilde u_1u_j}\Gamma^{\tilde\chi_1^0R}_{\tilde u_su_j}+C_0\Gamma^{\tilde gL*}_{\tilde u_1u_j}\Gamma^{\tilde\chi_1^0R}_{\tilde u_su_j}m_{\tilde g}m_{u_j}\\&+(C_0+C_{p_{\tilde u_1}})\Gamma^{\tilde gL*}_{\tilde u_1u_j}\Gamma^{\tilde\chi_1^0L}_{\tilde u_su_j}m_{\tilde g}m_{\tilde\chi_1^0}\\&+C_{p_{\tilde u_1}}\Gamma^{\tilde gR*}_{\tilde u_1u_j}\Big(\Gamma^{\tilde\chi_1^0R}_{\tilde u_su_j}m_{\tilde u_1}^2+\Gamma^{\tilde\chi_1^0L}_{\tilde u_su_j}m_{u_j}m_{\tilde\chi_1^0}\Big)\Big)P_R\\&+(L\leftrightarrow R)\Big]\end{aligned} \tag{A9}$$

with the abbreviations

$$C_0\equiv C_0(m_{\tilde u_1}^2,m_{\tilde\chi_1^0}^2,0;m_{\tilde g}^2,m_{u_j}^2,m_{\tilde u_s}^2) \tag{A10}$$

$$C_2\equiv C_2(m_{\tilde u_1}^2,m_{\tilde\chi_1^0}^2,0;m_{\tilde g}^2,m_{u_j}^2,m_{\tilde u_s}^2) \tag{A11}$$

$$C_{p_{\tilde u_1}}\equiv C_{p_{\tilde u_1}}(m_{\tilde u_1}^2,m_{\tilde\chi_1^0}^2,0;m_{\tilde g}^2,m_{u_j}^2,m_{\tilde u_s}^2). \tag{A12}$$

$C_{p_{\tilde u_1}}$ is defined through the decomposition

$$\begin{aligned}&\frac{16\pi^2}{i}\frac{\mu^{2\varepsilon}e^{\gamma\varepsilon}}{(4\pi)^\varepsilon}\int\frac{d^d\ell}{(2\pi)^d}\\&\quad\times\frac{\ell^\mu}{[\ell^2-m_{\tilde g}^2][(\ell+p_{\tilde u_1})^2-m_{u_j}^2][(\ell+p_{u_2})^2-m_{\tilde u_s}^2]}\\&\quad=p^\mu_{\tilde u_1}C_{p_{\tilde u_1}}+p^\mu_{u_2}C_{p_{u_2}}\end{aligned} \tag{A13}$$

and is given by

$$\begin{aligned}&C_{p_{\tilde u_1}}(m_{\tilde u_1}^2,m_{\tilde\chi_1^0}^2,0;m_{\tilde g}^2,m_{u_j}^2,m_{\tilde u_s}^2)\\&\quad=\frac{1}{m_{\tilde\chi_1^0}^2-m_{\tilde u_1}^2}[B_0(m_{\tilde\chi_1^0}^2;m_{u_j}^2,m_{\tilde u_s}^2)-B_0(m_{\tilde u_1}^2;m_{\tilde g}^2,m_{u_j}^2)\\&\qquad+(m_{\tilde g}^2-m_{\tilde u_s}^2)C_0(m_{\tilde u_1}^2,m_{\tilde\chi_1^0}^2,0;m_{\tilde g}^2,m_{u_j}^2,m_{\tilde u_s}^2)].\end{aligned} \tag{A14}$$

### 4. Self-energies of quarks and squarks

In our approximation where we put $m_c=0$, the quark self-energy contribution with an internal squark and gluino is only needed at $p^2=0$:

$$\Sigma^{\tilde gLR}_{fi}=\frac{\alpha_s}{2\pi}W^{\tilde q}_{fs}W^{\tilde q\star}_{i+3,s}C_Fm_{\tilde g}B_0(0;m_{\tilde g}^2,m_{\tilde q_s}^2), \tag{A15}$$

$$\begin{aligned}\Sigma^{\tilde gLL}_{fi}&=\frac{\alpha_s}{2\pi}W^{\tilde q}_{fs}W^{\tilde q\star}_{i,s}C_FB_1(0;m_{\tilde g}^2,m_{\tilde q_s}^2)\\&=-\frac{\alpha_s}{4\pi}C_F\frac{1}{\varepsilon}\delta_{fi}+\text{finite}.\end{aligned} \tag{A16}$$

For the contribution with an internal quark and gluon we get (for arbitrary $p^2$)

$$\Sigma^{\tilde gLL,RR}_{fi}(p^2)=\frac{\alpha_s}{4\pi}C_F(d-2)B_1(p^2;m_{q_i}^2,0)\delta_{fi}, \tag{A17}$$

$$\Sigma^{\tilde gLR,RL}_{fi}(p^2)=\frac{\alpha_s}{4\pi}C_Fdm_{q_i}B_0(p^2;m_{q_i}^2,0)\delta_{fi}. \tag{A18}$$

For the squark self-energies there are three contributions: First, the contribution with internal gluino and quark

$$\begin{aligned}\Sigma^{\tilde g}_{\tilde u_s\tilde u_t}(p^2)&=\frac{\alpha_sC_F}{\pi}\{(W^{\tilde u*}_{js}W^{\tilde u}_{jt}+W^{\tilde u*}_{j+3,s}W^{\tilde u}_{j+3,t})(B_2(p^2;m_{\tilde g}^2,m_{u_j}^2)+p^2B_1(p^2;m_{\tilde g}^2,m_{u_j}^2))\\&\quad-m_{\tilde g}m_{u_j}(W^{\tilde u*}_{js}W^{\tilde u}_{j+3,t}+W^{\tilde u*}_{j+3,s}W^{\tilde u}_{jt})B_0(p^2;m_{\tilde g}^2,m_{u_j}^2)\}\\&=\frac{\alpha_sC_F}{\pi}\frac{1}{\varepsilon}\left[\left(m_{\tilde g}^2-\frac{p^2}{2}\right)\delta_{st}+(W^{\tilde u*}_{js}W^{\tilde u}_{jt}+W^{\tilde u*}_{j+3,s}W^{\tilde u}_{j+3,t})m_{u_j}^2-m_{\tilde g}m_{u_j}(W^{\tilde u*}_{js}W^{\tilde u}_{j+3,t}+W^{\tilde u*}_{j+3,s}W^{\tilde u}_{jt})\right]+\text{finite},\end{aligned} \tag{A19}$$

second, the contribution with internal squark and gluon

$$\Sigma^{g}_{\tilde{u}_s\tilde{u}_t}(p^2) = \frac{\alpha_s}{4\pi} C_F (2(p^2 + m^2_{\tilde{u}_s}) B_0(p^2; m^2_{\tilde{u}_s}, 0) - A_0(m^2_{\tilde{u}_s}))\delta_{st}, \tag{A20}$$

and finally the contribution with a squark tadpole

$$\Sigma^{\tilde{u}\,\tilde{u}}_{\tilde{u}_s\tilde{u}_t} = -\frac{\alpha_s}{4\pi} C_F \bigg( \delta_{st} A_0(m^2_{\tilde{u}_s}) \tag{A21}$$

$$-2\sum_{i,j=1}^{3}\sum_{s'=1}^{6} (W^{\tilde{u}\star}_{i+3s} W^{\tilde{u}}_{i+3s'} W^{\tilde{u}\star}_{js'} W^{\tilde{u}}_{jt} + W^{\tilde{u}\star}_{is} W^{\tilde{u}}_{is'} W^{\tilde{u}\star}_{j+3s'} W^{\tilde{u}}_{j+3t}) A_0(m^2_{\tilde{u}_{s'}}) \bigg) \tag{A22}$$

$$= -\frac{\alpha_s}{4\pi} C_F \frac{1}{\varepsilon} [\delta_{st} m^2_{\tilde{u}_s} \tag{A23}$$

$$-2\sum_{i,j=1}^{3}\sum_{s'=1}^{6} (W^{\tilde{u}\star}_{i+3s} W^{\tilde{u}}_{i+3s'} W^{\tilde{u}\star}_{js'} W^{\tilde{u}}_{jt} + W^{\tilde{u}\star}_{is} W^{\tilde{u}}_{is'} W^{\tilde{u}\star}_{j+3s'} W^{\tilde{u}}_{j+3t}) m^2_{\tilde{u}_{s'}}] + \text{finite}. \tag{A24}$$

For further useful information on self-energies and LSZ factors, see Ref. [91].


[1] S. Dimopoulos and G. Giudice, Naturalness constraints in supersymmetric theories with nonuniversal soft terms, Phys. Lett. B **357**, 573 (1995).
[2] G. Giudice and A. Romanino, Split supersymmetry, Nucl. Phys. **B699**, 65 (2004).
[3] M. E. Machacek and M. T. Vaughn, Two loop renormalization group equations in a general quantum field theory. 3. Scalar quartic couplings, Nucl. Phys. **B249**, 70 (1985).
[4] Y. Yamada, Two Loop Renormalization of Gaugino Masses in General Supersymmetric Gauge Models, Phys. Rev. Lett. **72**, 25 (1994).
[5] S. P. Martin and M. T. Vaughn, Two loop renormalization group equations for soft supersymmetry breaking couplings, Phys. Rev. D **50**, 2282 (1994).
[6] A. H. Chamseddine, R. L. Arnowitt, and P. Nath, Locally Supersymmetric Grand Unification, Phys. Rev. Lett. **49**, 970 (1982).
[7] C. Boehm, A. Djouadi, and M. Drees, Light scalar top quarks and supersymmetric dark matter, Phys. Rev. D **62**, 035012 (2000).
[8] J. R. Ellis, K. A. Olive, and Y. Santoso, Calculations of neutralino stop coannihilation in the CMSSM, Astropart. Phys. **18**, 395 (2003).
[9] C. Balazs, M. S. Carena, and C. Wagner, Dark matter, light stops and electroweak baryogenesis, Phys. Rev. D **70**, 015007 (2004).
[10] C. Balazs, M. S. Carena, A. Menon, D. Morrissey, and C. Wagner, The supersymmetric origin of matter, Phys. Rev. D **71**, 075002 (2005).
[11] J. Ellis, K. A. Olive, and J. Zheng, The extent of the stop coannihilation strip, Eur. Phys. J. C **74**, 2947 (2014).
[12] A. De Simone, G. F. Giudice, and A. Strumia, Benchmarks for dark matter searches at the LHC, J. High Energy Phys. 06 (2014) 081.
[13] M. S. Carena, M. Quiros, and C. Wagner, Opening the window for electroweak baryogenesis, Phys. Lett. B **380**, 81 (1996).
[14] M. S. Carena, M. Quiros, and C. Wagner, Electroweak baryogenesis and Higgs and stop searches at LEP and the Tevatron, Nucl. Phys. **B524**, 3 (1998).
[15] P. Huet and A. E. Nelson, Electroweak baryogenesis in supersymmetric models, Phys. Rev. D **53**, 4578 (1996).
[16] D. Delepine, J. Gerard, R. Gonzalez Felipe, and J. Weyers, A light stop and electroweak baryogenesis, Phys. Lett. B **386**, 183 (1996).
[17] M. Losada, The two loop finite temperature effective potential of the MSSM and baryogenesis, Nucl. Phys. **B537**, 3 (1999).
[18] M. Losada, Mixing effects in the finite temperature effective potential of the MSSM with a light stop, Nucl. Phys. **B569**, 125 (2000).
[19] V. Cirigliano, S. Profumo, and M. J. Ramsey-Musolf, Baryogenesis, electric dipole moments and dark matter in the MSSM, J. High Energy Phys. 07 (2006) 002.
[20] M. Carena, G. Nardini, M. Quiros, and C. Wagner, The baryogenesis window in the MSSM, Nucl. Phys. **B812**, 243 (2009).
[21] M. Laine, G. Nardini, and K. Rummukainen, Lattice study of an electroweak phase transition at $m_h$ 126 GeV, J. Cosmol. Astropart. Phys. 01 (2013) 011.
[22] G. Aad *et al.*, Search for squarks and gluinos with the ATLAS detector in final states with jets and missing

transverse momentum using $\sqrt{s} = 8$ TeV proton-proton collision data, J. High Energy Phys. 09 (2014) 176.

[23] C. Collaboration, Search for supersymmetry in hadronic final states using MT2 with the CMS detector at $\sqrt{(s)} = 8$ TeV (unpublished).

[24] S. Sekmen, Inclusive SUSY searches at the LHC, arXiv: 1405.4730.

[25] C. Collaboration, Measurement of WW production rate (unpublished).

[26] G. Aad *et al.*, Measurement of $W^+W^-$ production in pp collisions at $\sqrt{s} = 7$ TeV with the ATLAS detector and limits on anomalous WWZ and WW couplings, Phys. Rev. D **87**, 112001 (2013).

[27] J. M. Campbell, R. K. Ellis, and G. Zanderighi, Next-to-leading order predictions for $WW + 1$ jet distributions at the LHC, J. High Energy Phys. 12 (2007) 056.

[28] K. Rolbiecki and K. Sakurai, Light stops emerging in WW cross section measurements? J. High Energy Phys. 09 (2013) 004.

[29] D. Curtin, P. Meade, and P.-J. Tien, Natural SUSY in plain sight, Phys. Rev. D **90**, 115012 (2014).

[30] G. Aad *et al.*, Observation of a new particle in the search for the standard model Higgs boson with the ATLAS detector at the LHC, Phys. Lett. B **716**, 1 (2012).

[31] S. Chatrchyan *et al.*, Observation of a new boson at a mass of 125 GeV with the CMS experiment at the LHC, Phys. Lett. B **716**, 30 (2012).

[32] C. Wymant, Optimising stop naturalness, Phys. Rev. D **86**, 115023 (2012).

[33] U. Ellwanger, C. Hugonie, and A. M. Teixeira, The next-to-minimal supersymmetric standard model, Phys. Rep. **496**, 1 (2010).

[34] L. J. Hall, D. Pinner, and J. T. Ruderman, A natural SUSY Higgs near 126 GeV, J. High Energy Phys. 04 (2012) 131.

[35] P. Batra, A. Delgado, D. E. Kaplan, and T. M. Tait, The Higgs mass bound in gauge extensions of the minimal supersymmetric standard model, J. High Energy Phys. 02 (2004) 043.

[36] S. Chatrchyan *et al.*, Search for top-squark pair production in the single-lepton final state in pp collisions at $\sqrt{s} = 8$ TeV, Eur. Phys. J. C **73**, 2677 (2013).

[37] Search for direct top squark pair production in final states with one isolated lepton, jets, and missing transverse momentum in $\sqrt{s} = 8$ TeV $pp$ collisions using 21 fb$^{-1}$ of ATLAS data (unpublished).

[38] C. Collaboration, Search for supersymmetry in pp collisions at $\sqrt{(s)} = 8$ TeV in events with three leptons and at least one b-tagged jet (unpublished).

[39] T. A. Collaboration, Search for direct top squark pair production in final states with two leptons in $\sqrt{s} = 8$ TeV pp collisions using 20 fb$^{-1}$ of ATLAS data (unpublished).

[40] G. Aad *et al.*, Search for top squark pair production in final states with one isolated lepton, jets, and missing transverse momentum in $\sqrt{s} = 8$ TeV pp collisions with the ATLAS detector, J. High Energy Phys. 11 (2014) 118.

[41] G. Aad *et al.*, Search for pair-produced third-generation squarks decaying via charm quarks or in compressed supersymmetric scenarios in $pp$ collisions at $\sqrt{s} = 8$ TeV with the ATLAS detector, Phys. Rev. D **90**, 052008 (2014).

[42] T. A. Collaboration, Search for pair-produced top squarks decaying into a charm quark and the lightest neutralinos with 20.3 fb$^{-1}$ of $pp$ collisions at $\sqrt{s} = 8$ TeV with the ATLAS detector at the LHC (unpublished).

[43] C. Collaboration, Search for top squarks decaying to a charm quark and a neutralino in events with a jet and missing transverse momentum (unpublished).

[44] R. S. Chivukula, H. Georgi, and L. Randall, A composite technicolor standard model of quarks, Nucl. Phys. **B292**, 93 (1987).

[45] L. Hall and L. Randall, Weak Scale Effective Supersymmetry, Phys. Rev. Lett. **65**, 2939 (1990).

[46] A. Buras, P. Gambino, M. Gorbahn, S. Jager, and L. Silvestrini, Universal unitarity triangle and physics beyond the standard model, Phys. Lett. B **500**, 161 (2001).

[47] G. D'Ambrosio, G. Giudice, G. Isidori, and A. Strumia, Minimal flavor violation: An effective field theory approach, Nucl. Phys. **B645**, 155 (2002).

[48] C. Bobeth, M. Bona, A. J. Buras, T. Ewerth, M. Pierini, L. Silvestrini, and A. Weiler, Upper bounds on rare K and B decays from minimal flavor violation, Nucl. Phys. **B726**, 252 (2005).

[49] G. Hiller and Y. Nir, Measuring flavor mixing with minimal flavor violation at the LHC, J. High Energy Phys. 03 (2008) 046.

[50] G. Hiller, J. S. Kim, and H. Sedello, Collider signatures of minimal flavor mixing from stop decay length measurements, Phys. Rev. D **80**, 115016 (2009).

[51] T. Han, K.-i. Hikasa, J. M. Yang, and X.-m. Zhang, The FCNC top squark decay as a probe of squark mixing, Phys. Rev. D **70**, 055001 (2004).

[52] S. Kraml and A. Raklev, Same-sign top quarks as signature of light stops at the LHC, Phys. Rev. D **73**, 075002 (2006).

[53] S. Bornhauser, M. Drees, S. Grab, and J. Kim, Light stop searches at the LHC in events with two b-jets and missing energy, Phys. Rev. D **83**, 035008 (2011).

[54] G. Belanger, D. Ghosh, R. Godbole, M. Guchait, and D. Sengupta, Probing the flavor violating scalar top quark signal at the LHC, Phys. Rev. D **89**, 015003 (2014).

[55] C. Boehm, A. Djouadi, and Y. Mambrini, Decays of the lightest top squark, Phys. Rev. D **61**, 095006 (2000).

[56] M. Muhlleitner and E. Popenda, Light stop decay in the MSSM with minimal flavour violation, J. High Energy Phys. 04 (2011) 095.

[57] K.-i. Hikasa and M. Kobayashi, Light scalar top at $e + e-$ colliders, Phys. Rev. D **36**, 724 (1987).

[58] S. Kraml, H. Eberl, A. Bartl, W. Majerotto, and W. Porod, SUSY QCD corrections to scalar quark decays into charginos and neutralinos, Phys. Lett. B **386**, 175 (1996).

[59] A. Djouadi, W. Hollik, and C. Junger, QCD corrections to scalar quark decays, Phys. Rev. D **55**, 6975 (1997).

[60] W. Beenakker, R. Hopker, and P. Zerwas, SUSY QCD decays of squarks and gluinos, Phys. Lett. B **378**, 159 (1996).

[61] W. Beenakker, R. Hopker, T. Plehn, and P. Zerwas, Stop decays in SUSY QCD, Z. Phys. C **75**, 349 (1997).

[62] M. Blanke, G. F. Giudice, P. Paradisi, G. Perez, and J. Zupan, Flavoured naturalness, J. High Energy Phys. 06 (2013) 022.

[63] A. Bartl, H. Eberl, E. Ginina, B. Herrmann, K. Hidaka, W. Majerotto, and W. Porod, Flavor violating bosonic squark decays at LHC, Int. J. Mod. Phys. A **29**, 1450035 (2014).

[64] P. Agrawal and C. Frugiuele, Mixing stops at the LHC, J. High Energy Phys. 01 (2014) 115.

[65] J. Aebischer, in *Proceedings of SUSY2014, The 22nd International Conference on Supersymmetry and Unification of Fundamental Interactions*, http://indico.hep.manchester.ac.uk/getFile.py/access?contribId=219&sessionId=22&resId=0&materialId=slides&confId=4221.

[66] R. Grober, M. Muhlleitner, E. Popenda, and A. Wlotzka, Light stop decays: Implications for LHC searches, arXiv:1408.4662.

[67] A. Crivellin, L. Hofer, and J. Rosiek, Complete resummation of chirally-enhanced loop-effects in the MSSM with non-minimal sources of flavor-violation, J. High Energy Phys. 07 (2011) 017.

[68] T. Banks, Supersymmetry and the quark mass matrix, Nucl. Phys. **B303**, 172 (1988).

[69] L. J. Hall, R. Rattazzi, and U. Sarid, The top quark mass in supersymmetric SO(10) unification, Phys. Rev. D **50**, 7048 (1994).

[70] R. Hempfling, Yukawa coupling unification with supersymmetric threshold corrections, Phys. Rev. D **49**, 6168 (1994).

[71] M. S. Carena, M. Olechowski, S. Pokorski, and C. Wagner, Electroweak symmetry breaking and bottom-top Yukawa unification, Nucl. Phys. **B426**, 269 (1994).

[72] T. Blazek, S. Raby, and S. Pokorski, Finite supersymmetric threshold corrections to CKM matrix elements in the large tan beta regime, Phys. Rev. D **52**, 4151 (1995).

[73] C. Hamzaoui, M. Pospelov, and M. Toharia, Higgs mediated FCNC in supersymmetric models with large tan beta, Phys. Rev. D **59**, 095005 (1999).

[74] M. S. Carena, D. Garcia, U. Nierste, and C. E. Wagner, Effective Lagrangian for the $\bar{t}bH^+$ interaction in the MSSM and charged Higgs phenomenology, Nucl. Phys. **B577**, 88 (2000).

[75] A. J. Buras, P. H. Chankowski, J. Rosiek, and L. Slawianowska, $\Delta M_{d,s}, B^0 d, s \to \mu^+\mu^-$ and $B \to X_s\gamma$ in supersymmetry at large $\tan\beta$, Nucl. Phys. **B659**, 3 (2003).

[76] L. Hofer, U. Nierste, and D. Scherer, Resummation of tan-beta-enhanced supersymmetric loop corrections beyond the decoupling limit, J. High Energy Phys. 10 (2009) 081.

[77] A. Crivellin, Effective Higgs vertices in the generic MSSM, Phys. Rev. D **83**, 056001 (2011).

[78] A. Bednyakov, A. Onishchenko, V. Velizhanin, and O. Veretin, Two loop $O(\alpha_s^2)$ MSSM corrections to the pole masses of heavy quarks, Eur. Phys. J. C **29**, 87 (2003).

[79] A. Bauer, L. Mihaila, and J. Salomon, Matching coefficients for $\alpha_s$ and $m_b$ to $O(\alpha_s^2)$ in the MSSM, J. High Energy Phys. 02 (2009) 037.

[80] D. Noth and M. Spira, Supersymmetric Higgs Yukawa couplings to bottom quarks at next-to-next-to-leading order, J. High Energy Phys. 06 (2011) 084.

[81] A. Crivellin and C. Greub, Two-loop SQCD corrections to Higgs-quark-quark couplings in the generic MSSM, Phys. Rev. D **87**, 015013 (2013).

[82] D. Noth and M. Spira, Higgs Boson Couplings to Bottom Quarks: Two-Loop Supersymmetry-QCD Corrections, Phys. Rev. Lett. **101**, 181801 (2008).

[83] L. Mihaila and C. Reisser, $O(\alpha_s^2)$ corrections to fermionic Higgs decays in the MSSM, J. High Energy Phys. 08 (2010) 021.

[84] H. E. Logan and U. Nierste, $B(s,d) \to \ell^+\ell^-$ in a two Higgs doublet model, Nucl. Phys. **B586**, 39 (2000).

[85] A. Crivellin and U. Nierste, Chirally enhanced corrections to FCNC processes in the generic MSSM, Phys. Rev. D **81**, 095007 (2010).

[86] A. Crivellin and J. Girrbach, Constraining the MSSM sfermion mass matrices with light fermion masses, Phys. Rev. D **81**, 076001 (2010).

[87] T. Huber and D. Maitre, HypExp: A Mathematica package for expanding hypergeometric functions around integer-valued parameters, Comput. Phys. Commun. **175**, 122 (2006).

[88] S. P. Martin, Two-loop scalar self-energies and pole masses in a general renormalizable theory with massless gauge bosons, Phys. Rev. D **71**, 116004 (2005).

[89] H. Asatrian, A. Hovhannisyan, and A. Yeghiazaryan, The phase space analysis for three and four massive particles in final states, Phys. Rev. D **86**, 114023 (2012).

[90] H. M. Asatrian and C. Greub, NLL QCD contribution of the electromagnetic dipole operator to $B \to X_s\gamma\gamma$ with a massive strange quark, Phys. Rev. D **89**, 094028 (2014).

[91] C. Greub, T. Hurth, V. Pilipp, C. Schupbach, and M. Steinhauser, Complete next-to-leading order gluino contributions to $b \to s\gamma$ and $b \to s +$ gluon, Nucl. Phys. **B853**, 240 (2011).